Brain Structure and Function (2020) 225:305–320
https://doi.org/10.1007/s00429-019-02003-7

ORIGINAL ARTICLE

Pupillary light reflex circuits in the Macaque Monkey: the olivary pretectal nucleus

Paul J. May[1,2,3] · **Susan Warren**[1]

Received: 10 September 2019 / Accepted: 5 December 2019 / Published online: 17 December 2019

Abstract

The olivary pretectal nucleus is the first central connection in the pupillary light reflex pathway, the circuit that adjusts the diameter of the pupil in response to ambient light levels. This study investigated aspects of the morphology and connectivity of the olivary pretectal nucleus in macaque monkeys by use of anterograde and retrograde tracers. Within the pretectum, the vast majority of neurons projecting to the preganglionic Edinger–Westphal nucleus were found within the olivary pretectal nucleus. Most of these neurons had somata located at the periphery of the nucleus and their heavily branched dendrites extended into the core of the nucleus. Retinal terminals were concentrated within the borders of the olivary pretectal nucleus. Ultrastructural examination of these terminals showed that they had clear spherical vesicles, occasional dense-core vesicles, and made asymmetric synaptic contacts. Retrogradely labeled cells projecting to the preganglionic Edinger–Westphal nucleus displayed relatively few somatic contacts. Double labeling indicated that these neurons receive direct retinal input. The concentration of retinal terminals within the nucleus and the extensive dendritic trees of the olivary projection cells provide a substrate for very large receptive fields. In some species, pretectal commissural connections are a substrate for balancing the direct and consensual pupillary responses to produce pupils of equal size. In the macaque, there was little evidence for such a commissural projection based on either anterograde or retrograde tracing. This may be due to the fact that each macaque retina provides nearly equal density projections to the ipsilateral and contralateral olivary pretectal nucleus.

Keywords Retinal projections · Pupil · Autonomic · Luminance · Midbrain

Abbreviations

At	Axon terminal
At*	Labeled axon terminal
BDA	Biotinylated dextran amine
CC	Caudal central subdivision
CG	Central gray
Den	Dendrite
Den*	Labeled dendrite
DLG	Dorsal lateral geniculate nucleus
DR	Dorsal raphe
EWpg	Preganglionic Edinger-Westphal nucleus
IC	Inferior colliculus
III	Oculomotor nucleus
InC	Interstitial nucleus of Cajal
IV	Trochlear nucleus
MD	Medial dorsal nucleus
MG	Medial geniculate nucleus
MLF	Medial longitudinal fasciculus
MPt	Medial pretectal nucleus
MRF	Midbrain reticular formation
nOT	Nucleus of the optic tract
nPC	Nucleus of the posterior commissure
OPt	Olivary pretectal nucleus
P	Pyramid
PAG	Periaqueductal gray
PC	Posterior commissure
PhaL	*Phaseolus vulgaris* leucoagglutinin
PRF	Pontine reticular formation
PPT	Posterior pretectal nucleus
Pt	Pretectum
Pul	Pulvinar
SGI	Intermediate gray layer

✉ Paul J. May
pmay@umc.edu

[1] Department of Neurobiology and Anatomical Sciences, University of Mississippi Medical Center, 2500 N. State St, Jackson, MS 39202, USA

[2] Department of Ophthalmology, University of Mississippi Medical Center, Jackson, MS, USA

[3] Department of Neurology, University of Mississippi Medical Center, Jackson, MS, USA

SGP	Deep gray layer
SN	Substantia nigra
SOA	Supraoculomotor area
Soma*	Labeled soma
WGA-HRP	Wheat germ agglutinin conjugated horseradish peroxidase

Introduction

If you walk down a sun-dappled path through a park, moving in and out of the shade, your eyes encounter large changes in ambient luminance, yet your visual capabilities are barely impacted by these changes, adapting seamlessly to the different light levels. This is partially due to the fact that cone photopigments have a fairly broad luminance range in which they function. However, the main player in the fast visual response to such luminance changes is the pupillary light reflex, in which the pupillary sphincter muscle of the iris quickly changes pupil diameter in response to central nervous system signals determined by luminance levels striking the retina (Gamlin 2006). This response, termed the pupillary light reflex, is generally believed to depend on a simple circuit in which the luminance input is provided by way of a projection from intrinsically photosensitive retinal ganglion cells (ipRGCs) containing melanopsin to a relay nucleus in the pretectum, the olivary pretectal nucleus (OPt) (Hattar et al. 2002; Schmidt et al. 2011; Hannibal et al. 2014). The OPt is believed to project directly to preganglionic motoneurons located in the Edinger–Westphal nucleus (EWpg) (Sun and May 2014b; Steiger and Büttner-Ennever 1979), which in turn supply the postganglionic parasympathetic motoneurons in the ciliary ganglion that innervate the pupillary sphincter muscle. This muscle forms a ring around the iridial margin (May et al. 2019). Electrical stimulation of the OPt produces pupillary constriction, reinforcing its role in the pupillary light reflex (rat—Trejo and Cicerone 1984; cat—Distler and Hoffmann 1989; macaque—Gamlin et al. 1995; Pong and Fuchs 2000). Generally, both pupils display the same pupillary diameter. Indeed, anisocoria, where the two pupils are not matched, is considered a clinically significant sign. The matched diameters are due to the presence of both a direct pathway for the pupillary light reflex circuit, connecting each retina with the ipsilateral pupillary sphincter muscle and a consensual pathway, connecting each retina to the contralateral pupillary sphincter muscle.

While the general features of the pupillary light reflex pathways are commonly accepted, many of the details of the circuit are not entirely clear and may differ between species. In particular, there has been little investigation of the circuitry in primates. Consequently, this report examines the portion of the pupillary light reflex circuitry that resides in the OPt of the macaque monkey. In cats, it has been shown that the pretectal neurons projecting to the EWpg receive direct retinal input (Sun and May 2014a). However, the organization of the OPt appears very different in cats and primates, so it is possible that the primate circuitry is more complex. Another area of investigation concerns the pathways that allow the direct and consensual pupillary light reflexes to be balanced. The presence of bilateral responses is believed to be due to three possible sites at which luminance information can cross the midline: the optic chiasm, commissural connections between the OPt nuclei, and the decussation of the pretectal–preganglionic axons in the posterior commissure (Simpson et al. 1988). In birds, which have entirely crossed projections from the retina to the pretectum, a specialized population of commissural pretectal neurons is present that tie the two nuclei together (Gamlin et al. 1984). In cats, where the crossed retinopretectal projection to OPt is denser than the ipsilateral projection, commissural pretectal neurons are also present in OPt (Sun and May 2014a). Monkeys display nearly equal projections from the retina of each eye to the two OPt (Hutchins and Weber 1985a), so it is possible that such a commissural projection is not necessary. This point has been investigated here. Portions of these data have been reported in brief formats (Sun and May 1995; May et al. 2008).

Methods

These experiments were performed in *Macaca fascicularis* monkeys ($N = 16$) (> 3.0 kg) of both sexes. Some of these cases were also used in other, non-conflicting studies. All procedures were performed in accordance with the dictates of the *Guide for Care and Use of Laboratory Animals* under protocols that were approved by the Institutional Animal Care and Use Committee for the University of Mississippi Medical Center. Animals were sedated by use of ketamine HCl (10 mg/kg, IM) and then anesthetized with inhaled isoflurane (3%). Ophthalmic proparacaine (0.5%) drops were applied to the cornea before intraocular injections. Butorphanol (0.01 mg/kg, IM) or Buprenex (0.001 mg/kg, IM) was given to provide analgesia after surgery. For perfusion, animals were again sedated with ketamine HCl and then deeply anesthetized with sodium pentobarbital (50 mg/kg, IP).

Injections

Edinger–Westphal nucleus injections In these animals (See Table 1 for details), an injection of wheat germ agglutinin conjugated horseradish peroxidase (WGA-HRP) was directed at the EWpg. First, the scalp was cut and retracted from the midline. Following a craniotomy, the underlying dura was incised to reveal the medial parietal cortex. This

Table 1 Injection details of cases used

Target	Tracer	Cases	Site #	Amount/site	Survival
Eye	1% WGA-HRP	3[a]	n.a	25–50 µl	2 days
EW	1% WGA-HRP	4[a]	1–3	0.03 µl	2 days
Pretectum	1% WGA-HRP	1	3	0.03 µl	1 day
Pretectum	4% Biocytin	2[a]	2–3	0.2 µl	1 day
Pretectum	10% BDA	4	1–2	0.1–0.4 µl	21 days
Pretectum	2.5% PhaL	2	1	n.a	14 days

[a]One animal received both a vitreal and EW injection

portion of cortex was aspirated to reveal the tentorium. Next, the aspiration of cortex was extended rostrally to reveal the dorsal surface of the superior colliculus, posterior surface of the pulvinar, pineal gland, and habenula. A 1 µl Hamilton syringe held by a micromanipulator with the needle tip rotated 2° medial in the frontal plane was used to make injections into the region containing the EWpg by inserting the needle just lateral to the habenula and rostral to the pineal. In some cases, an epoxy insulated Hamilton syringe was used to allow electrical stimulation of the oculomotor nucleus (III). The presence of eye movements following short trains of stimuli (5 ms burst with 20 square wave pulses/burst, < 1.0 mA stimulation) was used to indicate appropriate placement.

Intraocular injections To label retinal terminals in the OPt, WGA-HRP was injected into the vitreal cavity of the left eye of anesthetized animals (see Table 1). The solution was held in a 100 µl Hamilton syringe equipped with a 25G needle that was driven through the conjunctivum and underlying sclera to make the injection within the vitreous humor. Ophthalmic proparacaine drops were placed on the surface of the eye before inserting the needle. One of these animals also received an injection directed at the EWpg, as described above.

Pretectal injections To inject the OPt, the same approach was taken to reveal the surface of the midbrain, as described above. Four different tracers were used for these injections: WGA-HRP, biocytin, biotinylated dextran amine (BDA) (MW = 10,000), and *Phaseolus vulgaris* leukoagglutinin (PhaL) in pH 8.0 phosphate buffer (see Table 1). The first three tracers were injected using a 1 µl Hamilton syringe, and the last was injected iontophoretically using a glass micropipette with a 25 µm tip (7 µA, for 10 min, 50% duty cycle positive current). In each case, the needle or pipette was angled in the parasagittal plane between 23° and 30° tip rostral from vertical. The needle tip was directed just rostral to the blood vessel that runs at the border between the collicular and pulvinar surfaces. A region 3–4 mm off the midline and 1–2 mm beneath the surface was targeted in injections directed at the OPt. A fixative solution containing 1–2% paraformaldehyde and 1.25–1.5% glutaraldehyde in 0.1 M, pH 7.2 phosphate buffer (PB) was used in a transcardiac perfusion after a buffered saline rinse. The brains were blocked in the frontal plane and postfixed for a minimum of 1 h in the same solution, and then stored in 0.1 M, pH 7.2 PB at 4 °C.

Histological procedures

The brainstems were cut into 50 or 100 µm sections on a vibratome or freezing stage microtome. In the latter case, the brain was first sunk in 30% sucrose in 0.1 M, pH 7.2 PB as a cryoprotectant. At a minimum, a 1 in 3 series of sections was reacted to reveal the tracer. *WGA-HRP procedure* To reveal the location of WGA-HRP, a variation on the procedure of Olucha was used (Olucha et al. 1985; May et al. 1997). Sections were rinsed in 0.1 M, pH 6.0 PB, and then placed in a reaction solution consisting of 0.25% ammonium molybdate, 0.005% tetramethylbenzidine (TMB), and 2.5% ethanol in 0.1 M, pH 6.0 PB. The reaction was initiated by addition of H_2O_2 to achieve a concentration of 0.0125% and ran overnight at 4 °C. The blue reaction product was then stabilized by treatment in 5% ammonium molybdate in 0.1 M, pH 6.0 PB. *Biocytin and BDA procedure* (Chen and May 2000) Sections were rinsed in a solution containing 0.3% Triton-X-100 in 0.1 M, pH 7.2 PB. They were then incubated in a 1:500 solution of Avidin conjugated horseradish peroxidase (Avidin-HRP) (Vector Labs) in this Triton buffer for 20 h at 4 °C. Sections were rinsed in 0.1 M, pH 7.2 PB, and then reacted in a solution containing 0.5% diaminobenzidine (DAB), 0.005% cobalt chloride, and 0.01% nickel ammonium chloride in 0.1 M, pH 7.2 PB, with 0.005% H_2O_2 added to initiate the reaction. The reaction was halted by rinsing in 0.1 M, pH 7.2 PB. *PhaL procedure* (*after* Gerfen and Sawchenko 1984) Sections were rinsed in 0.3% Triton-X-100 and 10% normal goat serum in 0.1 M, pH 7.2 PB to increase permeability and decrease non-specific binding, respectively. They were then incubated overnight in 1:200 biotinylated goat anti-PhaL (Vector labs) in the Triton X-100, goat serum PB solution at 4 °C. The goat antibody was then localized using a goat ABC kit (Vector Labs), and the HRP was visualized by use of DAB as a chromagen, as described above. In all these cases, sections were mounted out of PB onto subbed glass slides, counterstained with cresyl violet, cleared in toluene, and coverslipped.

For EM analysis of WGA-HRP labeled cells and terminals, a second series of sections was processed with TMB, as described above. The blue TMB chromagen was further protected as follows. Sections were briefly rinsed in 0.1 M, pH 7.2 PB. They were then incubated in a solution containing 0.5% diaminobenzidine (DAB), 0.005% cobalt chloride, and 0.01% nickel ammonium chloride in 0.1 M, pH 7.2 PB. H_2O_2 was added to a concentration of 0.005% to initiate the reaction, which produced a black chromagen. The OPt was

cut out of free-floating sections under a Wild M-8 stereoscope. Samples containing the OPt were then prepared for electron microscopy (EM) using standard procedures (Barnerssoi and May 2016). Semithin sections were used to direct retrimming the blocks to areas of interest. Ultrathin sections were viewed and photographed using a Zeiss EM10C electron microscope.

For illustration, low magnification drawings of sections were done with a Wild M-9 stereoscope equipped with a drawing tube. Higher magnification drawings of labeled elements were made with an Olympus BH-2 microscope equipped with a drawing tube. Photomicrographs were taken with a Nikon Eclipse E600 photomicroscope equipped with a Nikon DS-Ri1 camera and Nikon Elements software on an attached PC. Adobe Photoshop was used to assemble the figures. The luminance, contrast, and color balance of the images were adjusted to match the microscopic appearance of the material.

Results

Olivary pretectal projection cells and retinal inputs

Figure 1a–c shows a WGA-HRP injection of III and the overlying supraoculomotor area (SOA). In macaques, the EWpg are embedded within the SOA. Within the pretectum (Fig. 1d–g), labeled cells (dots) were observed throughout the OPt on both sides. The labeled cells tended to be located near the edge of the nucleus. A small number of labeled cells were found dorsomedial to OPt, in the nucleus of the optic tract (nOT) (Fig. 1d,e,g). Additionally, a few other retrogradely labeled neurons were observed in the posterior pretectal (PPt) (Fig. 1e) and medial pretectal (MPt) nuclei (Fig. 1f). Since both EWpg nuclei were included in the injection, no statement on laterality can be made. The appearance of labeling in this case is further documented in Fig. 2. Large numbers of retrogradely labeled cells are apparent in OPt under crossed polarizer illumination (Fig. 2b, d). In addition, a distinct patch of labeled terminals (arrow) is present. It begins within the medial aspect of the nucleus and extends medially into nucleus of the optic tract (nOT) (Fig. 2b). A few retrogradely labeled neurons are associated with this patch. More labeled punta were present within the core of OPt (Fig. 2d, arrow). This terminal field indicates a projection from the area injected is present.

Figure 3a–c shows the extent of a second injection of WGA-HRP that included EWpg on both sides. The tracer essentially filled the area above III, where the SOA and the EWpg are located. The injection site extended into the left central gray (CG) with slight involvement of nucleus of the posterior commissure (nPC). The distribution of retrogradely labeled pretectal neurons (dots) can be observed in the higher magnification drawing (Fig. 3d). Labeled cells were present bilaterally in the OPt, as in Fig. 1. Additionally, they were scattered in the adjacent PPt ipsilateral to the injection. This animal also received an injection of WGA-HRP into the vitreous humor of the left eye. Intense anterograde label (stipple) was present bilaterally in the layers of dorsal lateral geniculate (DLG) (Fig. 3a, b) and in the pretectum (Fig. 3c, d). Within the pretectum, extremely dense anterograde terminal label was present in the OPt. Qualitatively, this nucleus displayed about the same level of terminal concentration on both sides of the brain. Numerous labeled terminals were also present within the nOT, but not in PPt. Thus, the pretectal region with the most extensive overlap between anterograde and retrograde labeling was the OPt. The pattern of labeling in this case is further illustrated in Fig. 4. In 4A, illumination with crossed polarization reveals the retinal terminal fields in the nOT and in the OPt. The latter terminal field entirely filled this ovoid nucleus and shows a mediodorsal extension, as well. Terminals were not present in the PPt. In Fig. 4b, bright-field illumination allows observation of both the anterogradely labeled terminal boutons and the retrogradely labeled neurons (arrowheads) in the OPt of this case. The retrogradely labeled cells definitely sit within the retinal terminal field.

Samples that included the OPt were taken from this case and prepared for electron microscopy. Figure 5 shows the ultrastructure of the labeled elements. Electron-dense flocculent TMB crystals (arrow) were present in the somata of retrogradely labeled neurons (Fig. 5a) and in their dendrites (Fig. 5b). The retrogradely labeled somata (Soma*) displayed nuclei with euchromatic nucleoplasm and indented nuclear membranes. Their plasma membranes had relatively few axosomatic contacts (arrowhead). In contrast, much of the surface of the retrogradely labeled dendrites (Den*) was covered by terminal profiles that made synaptic contact (arrowheads) with their membranes. Profiles that displayed symmetric synaptic densities and that displayed asymmetric synaptic densities were both observed contacting labeled dendrites. Anterogradely labeled terminals could also be identified by the presence of electron-dense crystals (Fig. 5c–e). These labeled terminals (At*) contained spherical vesicles. While the synaptic densities (arrowheads) varied in their appearance, the best presented ones appeared to make modest asymmetric synaptic contacts (Fig. 5d, e). They were occasionally observed contacting somata (Fig. 5c, d), but contacts on smaller dendrites (Fig. 5e) were much more common.

Figure 6 shows examples in which anterogradely labeled terminals were observed contacting retrogradely labeled profiles. The low magnification view (Fig. 6a) shows a primary dendrite (Den*) extending from the soma (Soma*) of a labeled cell. The electron-dense flocculent reaction product is indicated by arrows. Three

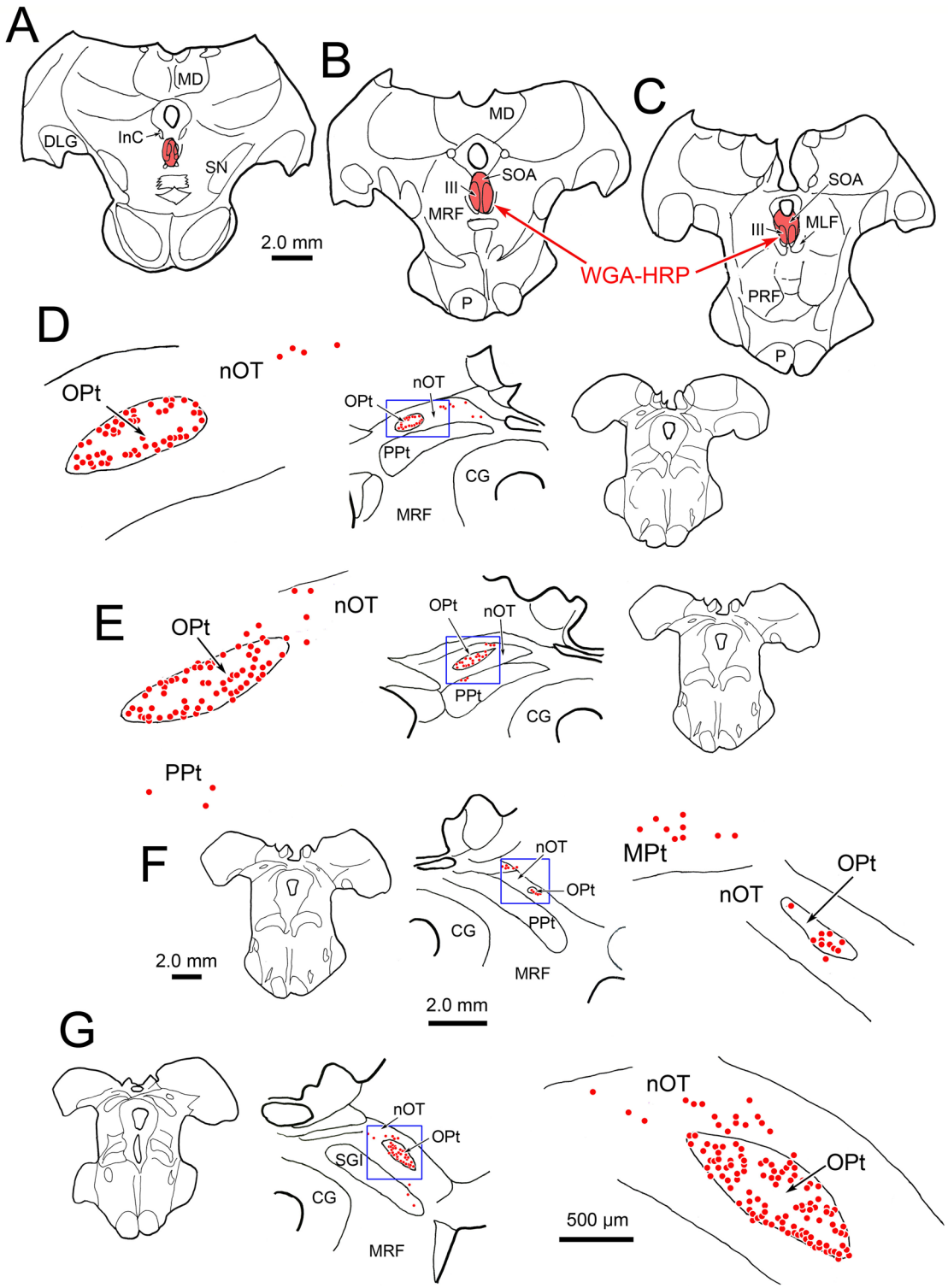

Fig. 1 Distribution of pretectal neurons supplying the EWpg. **a–c** The WGA-HRP injection site (red shading) included III and the area dorsal to it, the SOA. The EWpg is embedded within the SOA. Within the pretectum, most of the retrogradely labeled neurons (red dots) were found in OPt on both the left (**d**, **e**) and right (**f**, **g**) sides of the brainstem. A few scattered labeled cells were observed in the nOT (**d–g**), PPt (**e**), and MPt (**f**). In **d–g**, a low magnification drawing provides insight into the frontal section illustrated and a medium magnification drawing shows the area sampled (box) for the higher magnification charting

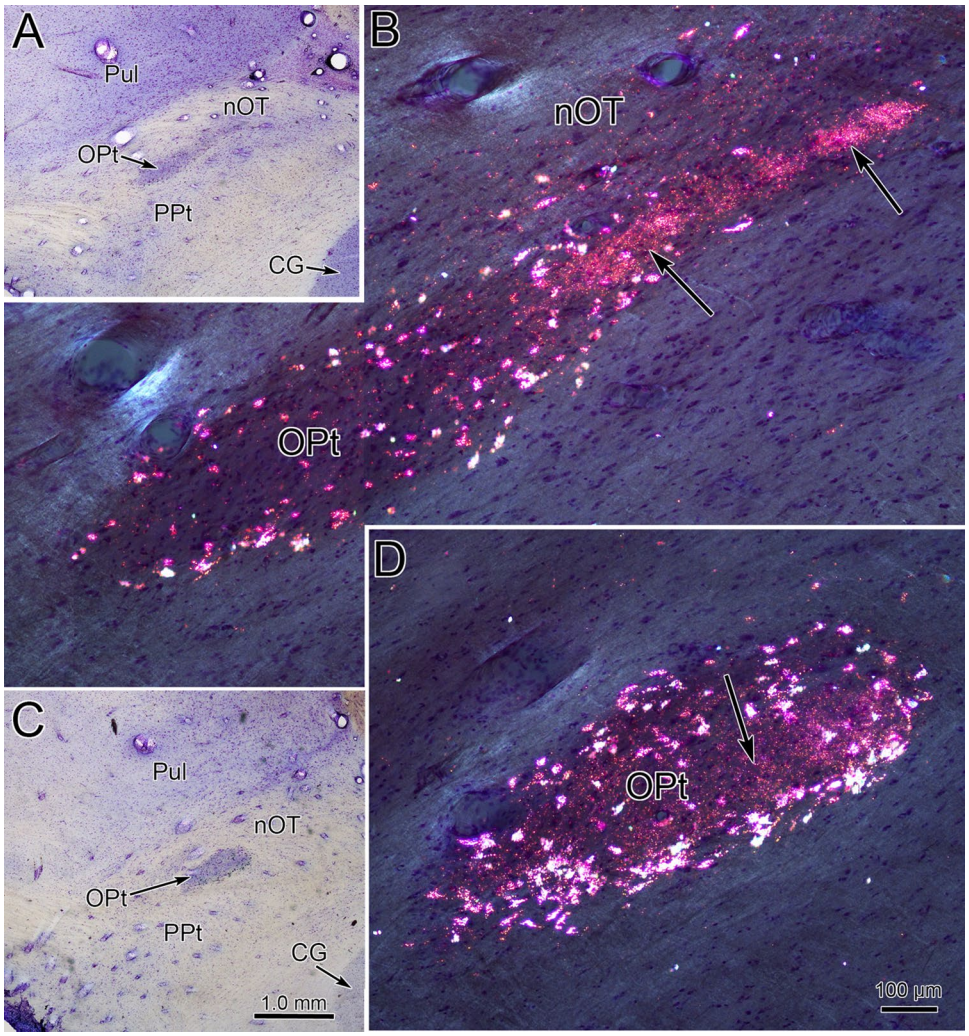

Fig. 2 Pattern of labeling in OPt following an injection including the EWpg. Two examples (**b**, **d**) of the labeling following the injection shown in Fig. 1 are presented using crossed polarizer illumination. Most of the labeled cells are located within OPt and tend to be found along the outer edge of the nucleus. Scattered cells are present in nOT. In **b**, a dense band of labeled terminals (arrows) begins in the medial corner of the nucleus and extends more medially. In **d**, more sparsely distributed labeled puncta (arrow) are found within the core of the OPt. Low magnification bright-field views (**a**, **c**) are provided to show the location of the higher magnification pictures (**b**, **d** respectively). Scale in **c** = **a**, **d** = **b**

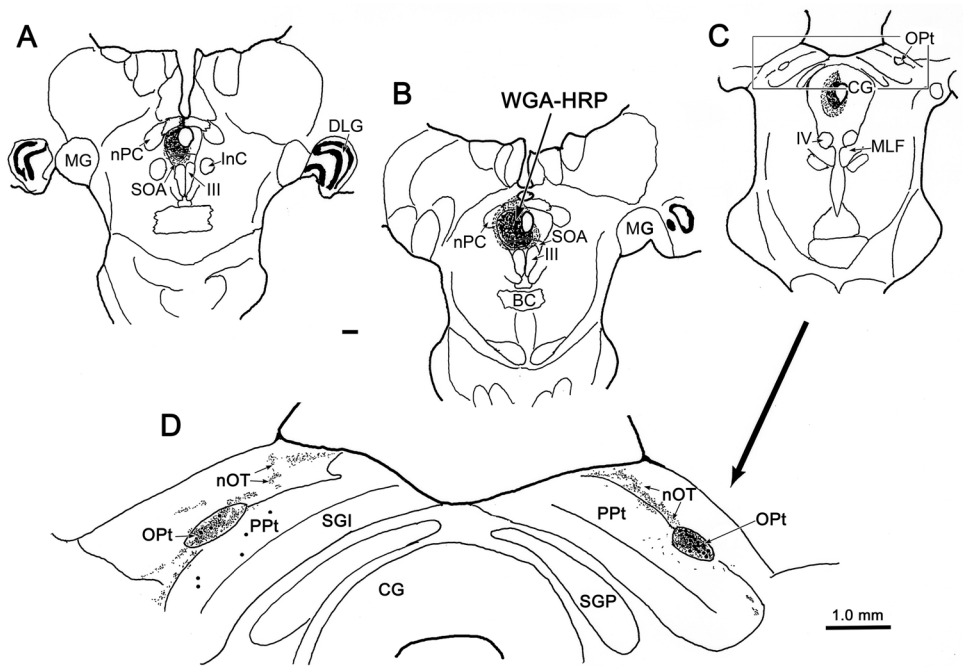

Fig. 3 Retinal terminals and premotor neurons overlap in OPt. **a**–**c** A WGA-HRP injection site (gray shading) located in the SOA, which contains the EWpg. The injection site spread along the track into the left CG, slightly involving the posterior commissure and nPC, but largely avoiding III. The boxed area in **c** is shown at higher magnification in **d**. Most of the retrogradely labeled neurons (dots) were located in the OPt, although a few were scattered in nOT and PPt. WGA-HRP was also injected into the vitreous humor of the left eye in this animal. It produced dense terminal labeling (stipple) in the nOT and OPt on both sides of the midbrain. Scale bar for **a**–**c** = 1.0 mm

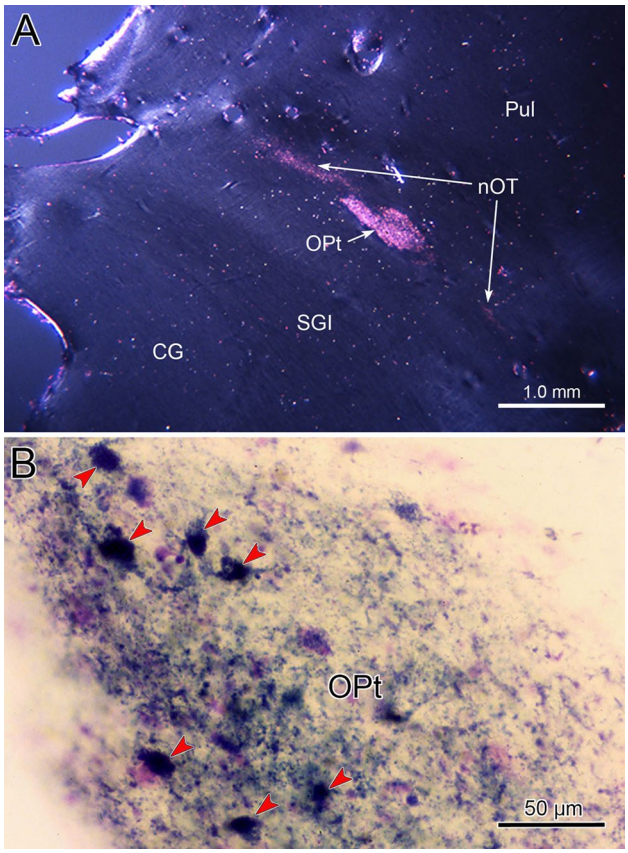

Fig. 4 Overlapping distribution of retinal terminals and olivary output neurons. **a** Crossed polarizer illumination reveals the distribution of retinal terminals within OPt and nOT following a vitreal injection of WGA-HRP in the contralateral eye. **b** In a bright-field, higher magnification view of the section shown in **a**, retrogradely label neurons (red arrowheads) sit within a dense field of anterogradely labeled terminals. The central injection producing the retrograde label is shown in Fig. 3

terminal profiles contacting (arrowheads) the junction of the dendrite and soma are shown at higher magnification (Fig. 6b–d). All three contain electron-dense crystalline material, indicating that they are anterogradely labeled terminals (At*). They are packed with clear, spherical synaptic vesicles, and two of the examples also contain a number of mitochondria. In some cases, a few dense-core vesicles (short arrows) were present, as well. Examples in which both the presynaptic and postsynaptic profile were labeled were also present in the neuropil. In Fig. 6e, an anterogradely labeled axon terminal (At*) is in synaptic contact (arrowheads) with both a large diameter dendrite (Den*) with crystalline reaction product (arrow) and a spine (Sp*) extending from this dendrite. These terminals were modestly asymmetric (Fig. 6d inset). In Fig. 6f, the labeled terminal contacts a smaller diameter labeled dendrite. This plate shows several examples of unlabeled, electron-lucent terminals (At) for comparison with the labeled examples, where the reaction product often obscures the ultrastructure.

Olivary pretectal neuron morphology

In two cases, the BDA injections placed in the pretectum were located medial to the OPt and extended through all the layers from the surface to the central gray. Consequently, they involved crossing fibers of the posterior commissure (Fig. 7 inserts). This injection location produced homogeneous filling of the neurons in the OPt. Ipsilateral to the injection, virtually, all the OPt neurons were fully labeled, making it difficult to follow the dendrites of individual neurons. Since fewer cells were labeled contralaterally, we illustrated these examples (Fig. 7a–d). The labeled OPt neurons were multipolar, and in better labeled examples, it was observed that their dendrites branched multiple times. Nearly all of their dendritic tree extended within the OPt and avoided the surrounding neuropil. In sections through the middle of the nucleus (Fig. 7b, c), it could be seen that the labeled cell somata tended to be located near the edge of the nucleus with their dendrites extending into the core of OPt. This may be true of the rostral (Fig. 7a) and caudal (Fig. 7d) poles as well, but this organization may not be visible in frontal sections, as the core of the nucleus would be located caudal or rostral to each pole, respectively. The actual appearance of the OPt in Fig. 7c is shown in Fig. 8a. The higher magnification views (Fig. 8b, c) provide an even better appreciation of the extensive dendritic fields of these cells, which are reminiscent of Purkinje cells.

Investigation of non-retinal inputs

It was not clear whether the cells shown in Figs. 7 and 8 were labeled, because they projected to the contralateral OPt or because their axons were labeled after they crossed the midline on their way to the EWpg. To directly address the question of OPt commissural projections in the macaque, we examined cases in which the injection site involved the OPt. Figure 9 shows an example of a large WGA-HRP injection that included the OPt, as well as most of PPt and nOT, with spread into the overlying pulvinar (Fig. 9a–f). A large band of labeled axons (lines) crossed the posterior commissure (PC) (Fig. 9a–d). Some of these terminated in the nucleus of the posterior commissure (nPC) (Fig. 9a–c). Others extended laterally into the rest of the pretectum. This injection produced considerable terminal (stipple) and cellular (dots) label in the contralateral nOT (Fig. 9b–e). The anterior pretectal nucleus (APt) contained several labeled cells (Fig. 9c), and the PPt showed sparse terminal label and scattered retrogradely labeled neurons (Fig. 9d, e). However, the labeled terminals largely avoided the OPt, and labeled neurons were not

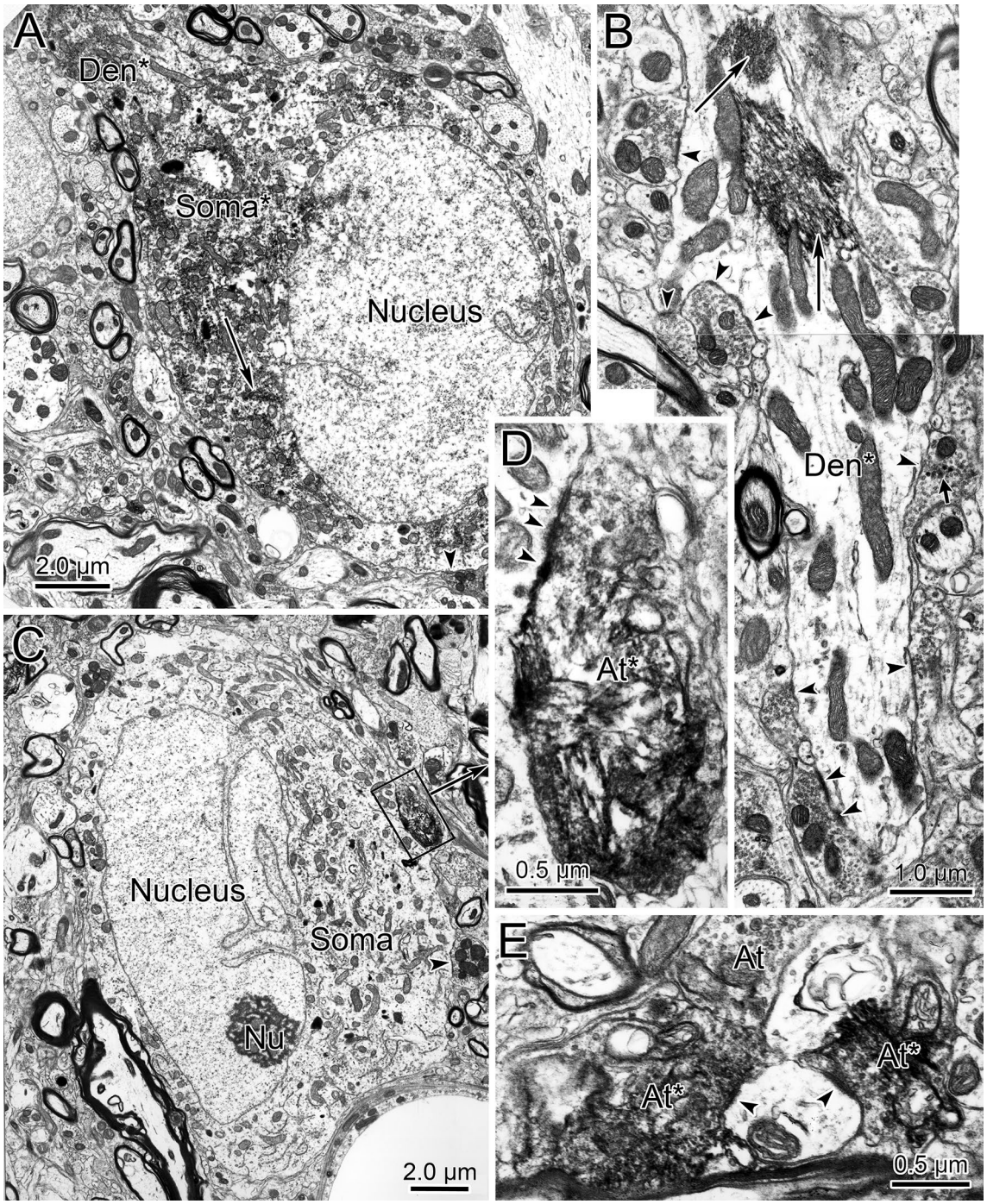

Fig. 5 Ultrastructure of labeled elements (asterisk) in the OPt. Electron microscopic examination of tissue from the case shown in Figs. 3 and 4 reveals the presence of retrogradely labeled premotor neuron somata (Soma*) (**a**) and dendrites (Den*) (**b**). Profiles contacting them are indicated by arrowheads. Presumed retinal terminals were anterogradely labeled (**c**–**e**). The labeled axosomatic terminal (At*) in **d** contacts an unlabeled cell (Soma). Its location is shown by the box in **c**. Two anterogradely labeled terminals and an unlabeled terminal (At) contact an unlabeled dendrite (Den) in **e**. Arrowheads indicate synaptic contacts on these profiles. Arrows point to examples of electron-dense, crystalline reaction product in **a** and **b**

present within the nucleus (Fig. 9d, e). On the other hand, labeled cells were present in the nOT. Their location can be seen under crossed polarizer illumination (Fig. 10a, b). The numerous retrogradely labeled neurons (arrows) were distributed right up to the border of, but not within, the OPt (Fig. 10b). Note the medial extension of the nuclear borders of OPt in this view (Fig. 10b) that matches the area of terminals observed in Fig. 2.

Labeled terminals were also largely absent from the contralateral OPt following pretectal BDA injections that included the OPt. An example of such a pretectal BDA injection that included all of OPt, and portions of nOT and PPt is shown in the insert in Fig. 10c. Following this large injection, only a few thin labeled axons (arrows) could be seen within the borders of the contralateral OPt (Fig. 10d). Similarly, pretectal injections of PhaL produced no labeled axon terminals in the contralateral OPt. However, these injections did not involve OPt. In one example, the injection site lay medial to OPt in nOT (Fig. 10e). In the other, the injection site lay ventral to OPt in PPt (Fig. 10g). While no contralateral label was seen (not illustrated), in both these cases, numerous labeled axons studded with *en passant* boutons were present in the adjacent, ipsilateral OPt (Fig. 10f, h).

Discussion

This is the first detailed study of the anatomy of the macaque OPt. The data presented here strongly suggest that the retinal projection to the macaque OPt terminates on output neurons that project to the EWpg. These retinal terminals have ultrastructural specializations that suggest they produce excitation and may also contain peptide co-transmitters. They preferentially target the dendrites of the output neurons. In fact, the output neuron somata tend to be found at the periphery of the nucleus and their extensive dendritic fields fill its core. This organization may underlie the large receptive fields of OPt cells. We found little evidence to indicate the two OPt are linked by a commissural projection in the macaque.

Retinal input

The presence of retinal input to the OPt is well known (rat—Scalia and Arango 1979; rabbit—Klooster et al. 1983; cat—Hoffmann et al. 1984; squirrel monkey—Hutchins and Weber 1985a; pigeon—Gamlin and Cohen 1988; bat—Scalia et al. 2015). The balanced pattern of ipsilateral and contralateral projections seen here in the macaque is similar to that observed in squirrel monkeys (Hutchins and Weber 1985a). We did not see any evidence of the lamellar pattern of inputs that was reported in that species, but we used a different tracer and did not cut the brain in the planes that best revealed this pattern (Weber et al. 1981). It is possible that some of the terminals that were labeled in the case with a second EWpg injection were central, not retinal, projections (Fig. 2d). However, comparison of Figs. 2 and 4 suggests that the retinal terminals far outnumbered this central population, making it unlikely that any individual terminal which we observed ultrastructurally was from this non-retinal source. The ultrastructure of the retinal terminals is similar to that reported in the rat and cat, with the terminals containing numerous clear, spherical vesicles, and making asymmetric synaptic contacts on OPt somata, dendrites, and spines (Campbell and Lieberman 1985; Klooster and Vrensen 1997; Sun and May 2014a). These terminals are characterized by pale mitochondria in other species, and mitochondria with relatively light matrix were observed in some of the macaque terminals (Fig. 6b, c). We also observed a few dense-core vesicles in these terminals, suggesting that, in addition to glutamate, they utilize peptide co-transmitters. In fact, substance P has been reported in OPt retinal terminals (rat—Miguel-Hildago et al. 1994; Klooster et al. 2000), as has pituitary adenylate cyclase-activating polypeptide (PACAP) (monkey—Hannibal et al. 2014). Complex glomerular arrangements including presynaptic dendrites, presumably from GABAergic interneurons, have been reported in the rodent OPt (Campbell and Lieberman 1982; Klooster and Vrensen 1997). Our limited ultrastructural analysis was directed at determining retinal pretectal connectivity, so we cannot comment on whether this organization was present in the monkey.

There is good evidence that the pupillary light reflex is driven by ipRCGs that contain melanopsin (Hattar et al. 2002; Ostrin et al. 2018). These melanopsin-containing cells, first described by Berson et al. (2002), receive input from photoreceptors, but are also capable of being directly activated by light (Schmidt et al. 2011). Since their discovery, it has become evident that there are several subtypes of ipRCGs that differ in the amount of melanopsin they express, their laminar dendritic distribution, and their photoreceptor inputs (Schmidt et al. 2011). Of these, two subtypes, whose dendrites differ in the sublamina of the outer plexiform layer in which they arborize, project to the macaque OPt (Hannibal et al. 2014; Liao et al. 2016). Both types are driven by on bipolar cells, but they likely differ with respect to their photoreceptor input. They share a general dendritic morphology in that they have very large, sparsely branched dendritic fields, but have relatively small somata. The latter places them in the koniocellular or K-type ganglion cell category that was physiologically defined as the W class of ganglion cells with very slow axon conduction velocities (Fukuda and Stone 1974). The terminal distribution of the ipRGCs in OPt correlates with that seen in the present study (Hannibal et al. 2014). These cells also provide input to the suprachiasmatic nucleus, so they may also contribute luminance information to the descending pathways that target preganglionic sympathetic motoneurons for the dark response (May et al. 2019).

Anterogradely labeled retinal terminals were observed to directly contact retrogradely labeled OPt output neurons that presumably supply the EWpg (Fig. 6). It is possible that the labeled neurons target other nuclei within the injection sites. However, there was some variation in the injection site location among our cases, and all the cases in which OPt contained labeled cells included the EWpg, the SOA and the

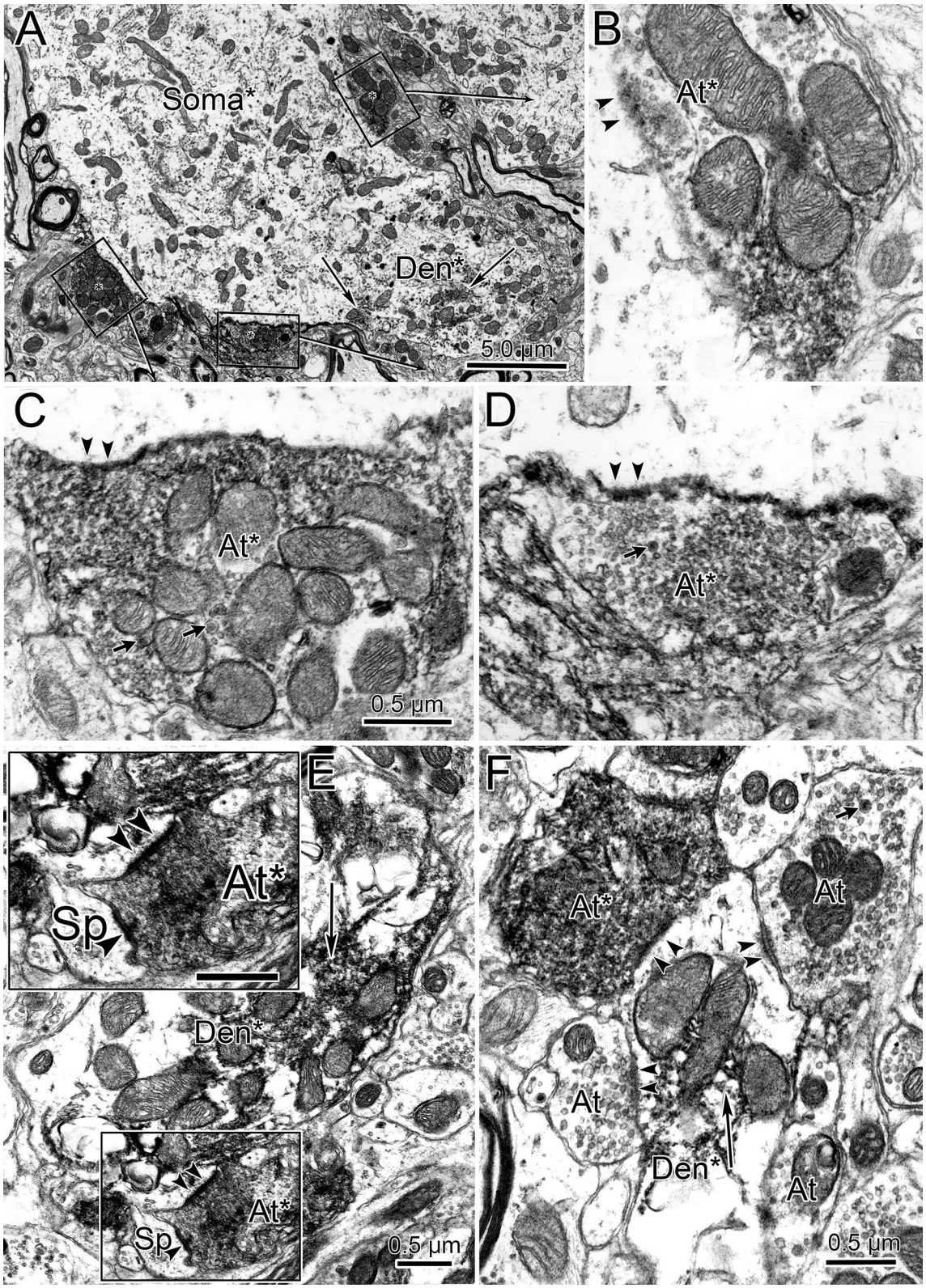

ventral central gray immediately adjacent to the SOA. OPt labeling was still present when other proposed targets of the OPt, such as the nucleus of Darkschewitsch or the nucleus of the posterior commissure (Klooster et al. 1995), were not included in the injection site. It has recently been shown that preganglionic motoneurons within EWpg extend their

◂**Fig. 6** Dual labeling indicates direct synaptic input by retinal terminals onto olivary output neurons. Electron microscopic examination of tissue from the case shown in Figs. 3 and 4 reveals the presence of anterogradely labeled terminals (At*) contacting a retrogradely labeled soma (Soma*) (**a**) and dendrites (Den*) (**a**, **e**, **f**). Arrows in **a**, **e,** and **f** indicate electron-dense, crystalline reaction product in the postsynaptic elements. Comparison between the labeled terminals (At*) and unlabeled ones (At) shows that the vesicles in the former are coated with an electron-dense fuzz. Boxes in **a** indicate the location of the terminals shown in **b–d**. The labeled terminals synaptically contact (arrowheads) the soma (**a–c**), dendrites (**d–f**), and even a spine (Sp) (**e**) of the retrogradely labeled cells. Details of the terminals in **e** (box) are shown at 50% higher magnification in the insert. Scale **c** = **b**, **d**

dendrites broadly in the SOA (May et al. 2018). Thus, spread into this region would still produce uptake by likely EWpg motoneurons afferents. The presence of a monosynaptic retinal input onto these OPt output neurons in the macaque mirrors findings in the cat (Sun and May 2014a), indicating that this direct input is a general mammalian feature. The ultrastructure of the output cells appears to be common as well, as an indented nucleus and relative lack of somatic contacts has been reported in the rat and cat (Klooster and Vrensen 1997; Sun and May 2014a).

Output neurons

The organization of the output neurons within the macaque OPt was noteworthy. Their somata tended to be located peripherally, and their well-arborized dendritic trees extended into the core of the nucleus. This peripheral somatic distribution was previously noted (Gamlin and Clarke 1995). The experiment that produced homogeneous filling of the OPt cell dendrites labeled these cells by fiber-of-passage uptake, so we cannot be sure of the targets of the labeled cells. However, their distribution is very similar to that of the cells labeled from injections that included EWpg. So it is likely that the homogeneously labeled neurons are similar, if not identical, to those of the light reflex pathway. The dendritic morphology of these cells is reminiscent of that shown with Golgi stains in the rat OPt (Gregory 1985; Campbell and Lieberman 1985), but somewhat different from that observed in the cat with retrograde labeling. Moreover, the cat OPt does not have an ovoid shape, and output cells are distributed across the nucleus. The output neurons are located near the periphery of the marmoset OPt, so this organization may be a primate feature (Clarke et al. 2003a).

The dendritic morphology of the OPt output cells may help to explain the receptive field characteristics of these neurons. Clarke et al. (2003b) divided macaque OPt cells into three types based on their receptive field characteristics: bilateral, contralateral, and macular. The bilateral and contralateral classes had receptive fields that covered much of the available visual field. They estimated that even the "macular cells", which had the smallest receptive fields, might receive inputs from as many as 100 retinal ganglion cells. Similarly, the cat OPt cells also have very large receptive fields (Distler and Hoffmann 1989). The combination of extensive OPt cell dendritic fields and the concentration of the retinal terminals within the small area represented by the OPt is likely to produce a large amount of retinal pretectal convergence, leading to these large receptive fields. OPt neurons generally show little difference in their firing with respect to the region of the receptive field stimulated. Instead, they fire in a tonic fashion that reflects the general luminance level. (Trejo and Cicerone 1984; Clark and Ikeda 1985a, b; Distler and Hoffmann 1989; Gamlin et al. 1995; Pong and Fuchs 2000). The anatomical substrate for convergence that we have shown here may also help support the capacity of these neurons to signal overall retinal luminance levels, effectively averaging out irregularities in luminance levels across the retina. How the retinal inputs are organized to produce the three different OPt classes seen in macaques (Clarke et al. 2003a, b) cannot be explained by the present results. That will require an analysis at the level of individual cells.

A medial extension of the ovoid OPt was observed (Fig. 10b). This region received a dense retinal projection (Fig. 4a) and also contained a considerable number of labeled terminals following injections of the SOA (Fig. 2b). Retrogradely labeled output neurons were not located within the borders of this region, but some were present immediately outside it (Figs. 1e, g, 2b). It is possible that, while nominally located within the nOT, these cells send dendrites into this terminal field and they are part of the pupillary light reflex circuit. An extension of the OPt was also described in the cat (Hutchins and Weber 1985b), and this region of retinal termination can be seen in the squirrel monkey, as well (Hutchins and Weber 1985a).

Non-retinal inputs

In pigeons, the retinal projection to the OPt is entirely crossed (Gamlin and Cohen 1988). In mammals with laterally placed eyes, the projection is also entirely crossed, or has just a small ipsilateral component (Scalia 1972; Scalia and Arango 1979; Klooster et al. 1983). These species exhibit a considerable commissural connection between the two OPt, presumably related to balancing the luminance information from the two eyes to produce equivalent direct and consensual pupillary responses (Gamlin et al. 1984; Klooster et al. 1995; Klooster and Vrensen 1997). The cat OPt receives a substantial ipsilateral retinal projection in line with its more frontally placed eyes, but still has a set of commissural neurons that are located in a separate subdivision of the nucleus (Sun and May 2014a). However, in the present study, we did not observe retrogradely

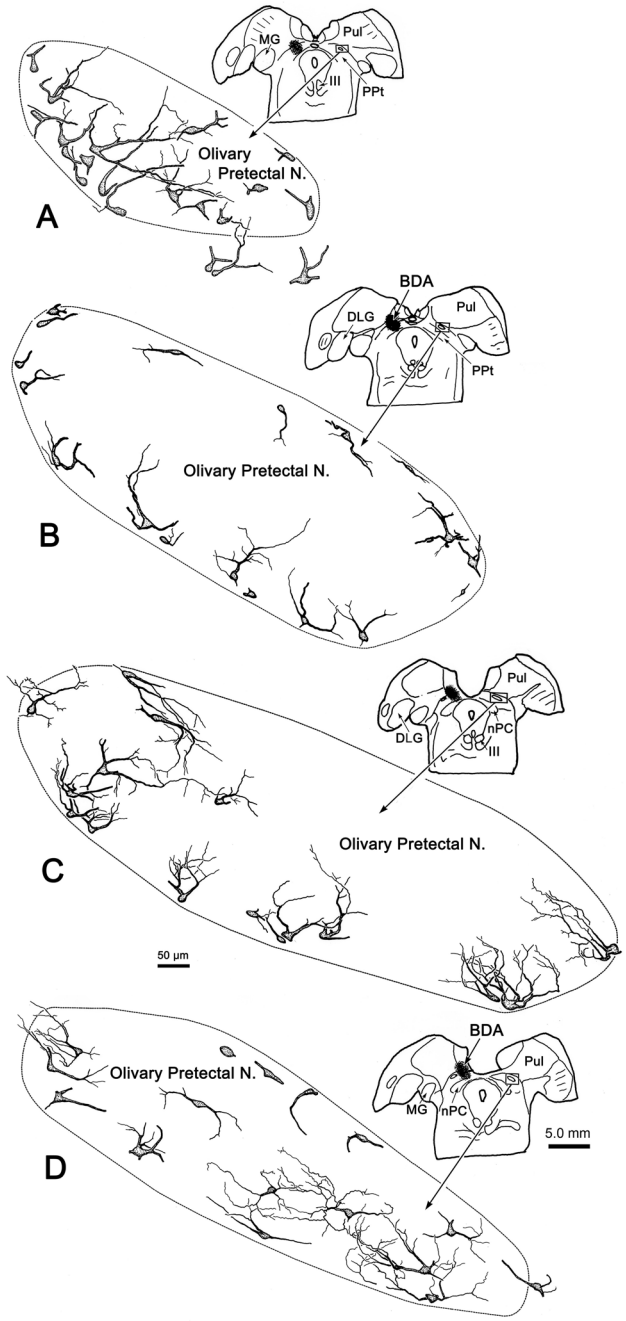

Fig. 7 Morphology and distribution of OPt output neurons. An injection of BDA located between OPt and the posterior commissure produced homogeneous labeling of neurons in the contralateral OPt whose axons crossed in the posterior commissure. A rostral-to-caudal series of low magnification drawings in **a**–**d** show the location of the injection site and the area sampled in the high magnification drawings. The high magnification drawings in **a**–**d** illustrate how most of the labeled cells have somata found near the external surface of the nucleus and send their dendrites extending toward the core of the nucleus

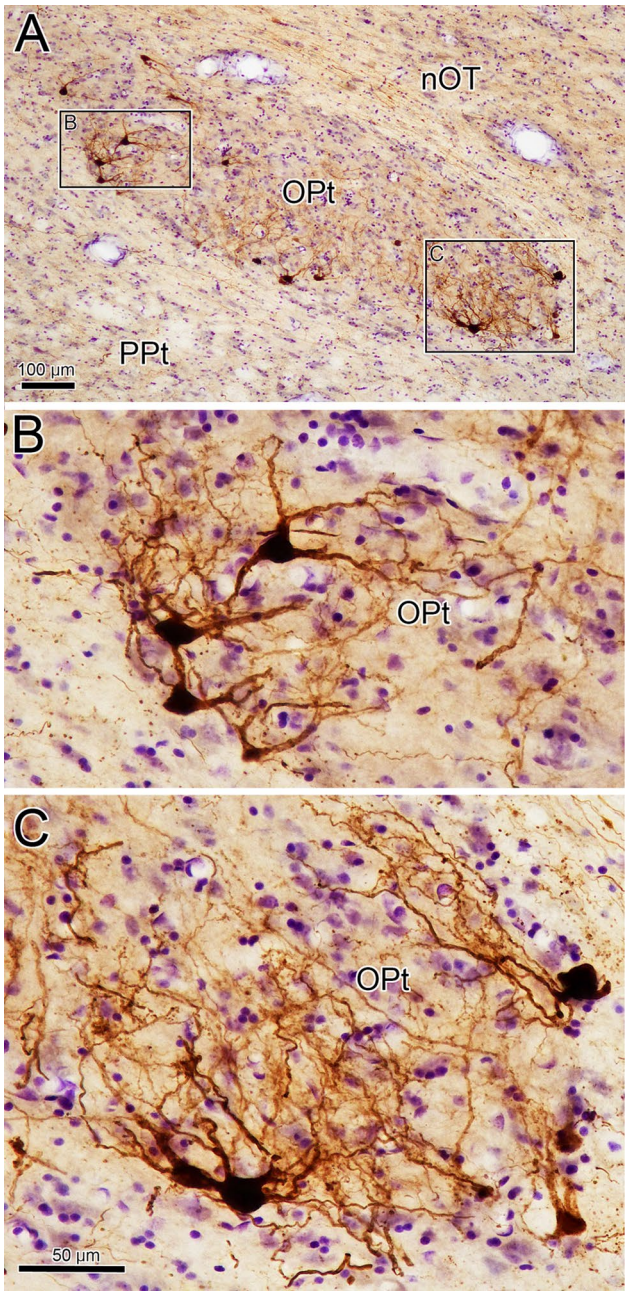

Fig. 8 Dendritic morphology of OPt output neurons. These homogeneously stained, brown neurons were labeled from the injection shown in Fig. 7 and are illustrated in Fig. 7c. They display multipolar somata from which several dendrites extend and branch several times within the confines of the nucleus. They do not extend toward the adjacent nOT or PPt. Location of higher magnification plates (**b**, **c**) is shown by boxes in the lower magnification view (**a**). Scale in **c** = **b**

labeled commissural neurons within the macaque OPt (Figs. 9, 10a, b), which matches a previous report (Mustari et al. 1994). It is possible that the commissural neurons lie outside the OPt within the nOT, as retrogradely labeled commissural neurons were present there. However, little or no anterograde label was present in the OPt following

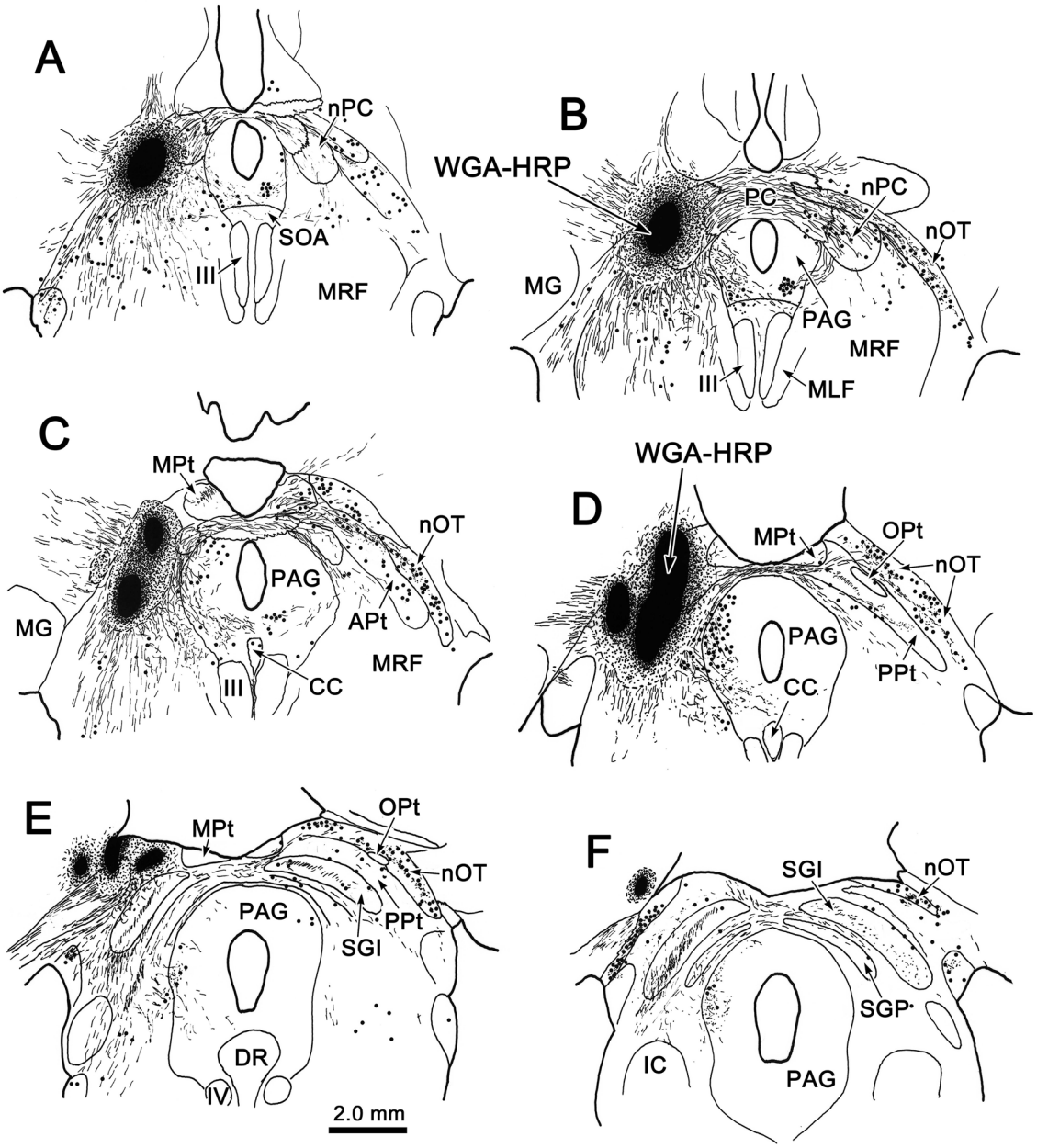

Fig. 9 Pretectal commissural projections. A large injection of WGA-HRP involved most of the pretectum (**a–e**). Large numbers of labeled axons (lines) were observed crossing in the PC (**b**, **c**), and terminal label (stipple) was found in the contralateral nPC (**a–c**), MPt (**c**, **d**), nOT (**b–f**), and PPt (**d**, **e**) of the pretectum, as well as in the SGI of the superior colliculus (**e**, **f**). Retrogradely labeled neurons (dots) were observed in the nPC (**a**, **b**), APt (**c**), nOT (**c–f**), and PPt (**d**, **e**). However, no labeled terminals or cells were found within the confines of the OPt (**d**, **e**)

injections that included the OPt and nOT or just the nOT (Fig. 10c–g). This agrees with the previous findings in the macaque (Baleydier et al. 1990). A commissural projection may not be necessary in a fully frontal-eye species like the macaque. As nearly equal projections from the ipsilateral and contralateral eyes are found within the OPt, no balancing of input for the direct and consensual pupillary responses may be needed.

The present study did demonstrate a considerable projection by the surrounding nOT and PPt into the ipsilateral OPt (Fig. 10e–h). Previous studies have also shown that the OPt receives input from nuclei in the accessory optic system (monkey—Baleydier et al. 1990; rat—Klooster et al. 1995), as well as from other parts of the brainstem oculomotor system (Lieberman et al. 1985; Gamlin 2006). The effects of these inputs are, to the best our knowledge,

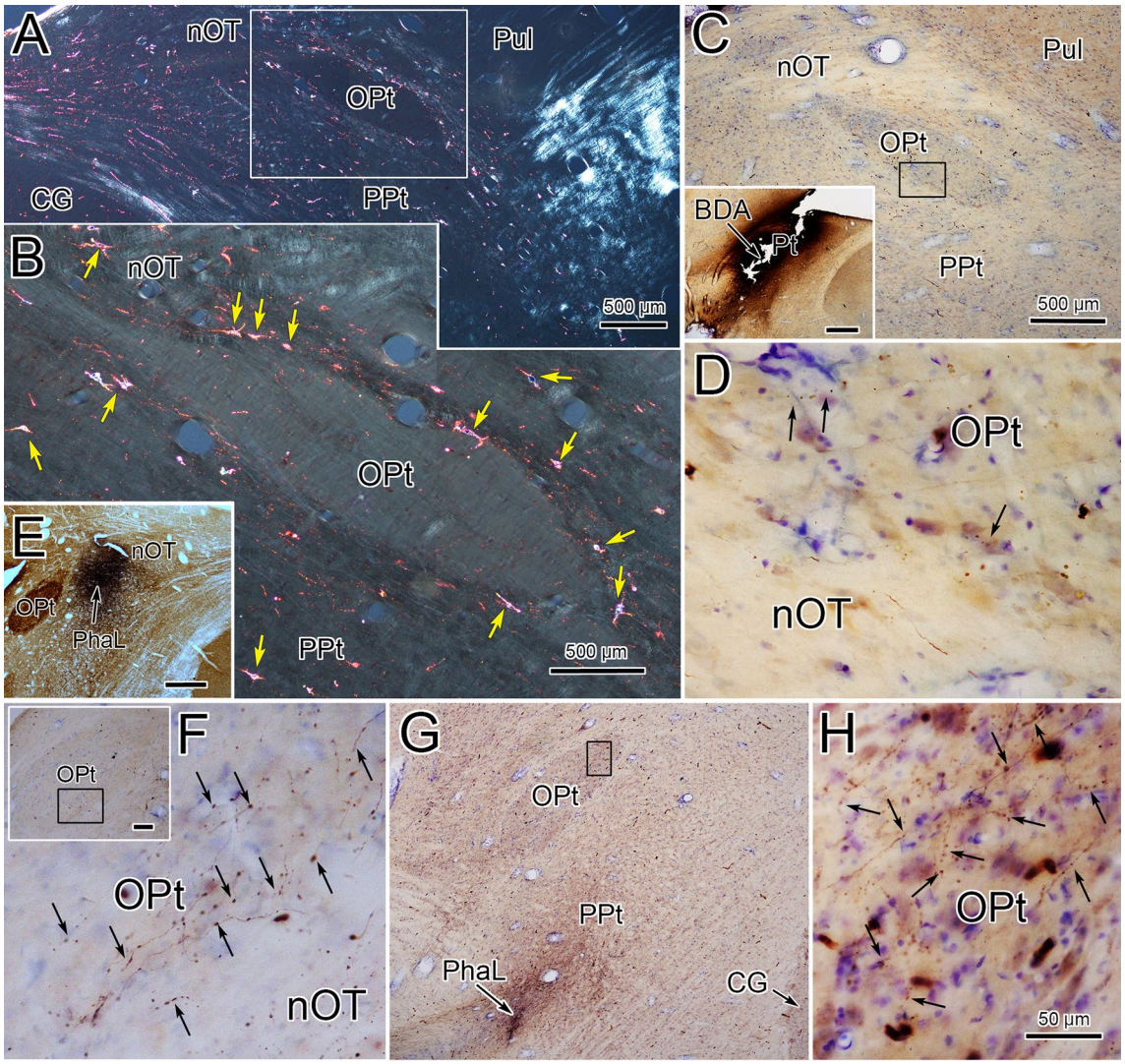

Fig. 10 Non-retinal input to the OPt. **a**, **b** Low and higher magnification view of the OPt using crossed polarizer illumination (box in **a** indicates sampled area in **b**). Following the large pretectal injection of WGA-HRP shown in Fig. 9, numerous retrogradely labeled neurons (yellow arrows) were observed in nOT, immediately outside the borders of the OPt, and in PPt, but labeled cells were not located within OPt. **c**, **d** A large BDA injection of the pretectum that included OPt (inset in **c**) led to light labeling of just a few axons (arrows) lying within the OPt (**d**) (box in **c** indicates location of **d**). **e**, **f** A PhaL injection into the nOT (**e**) did not produce any terminal label in the contralateral OPt (not shown), but produced an extensive plexus of labeled axons (arrows) in the adjacent ipsilateral OPt (**f**) (box in inset indicates the location of **f**). **g**, **h** Similarly, a PhaL injection into the PPt (**g**) did not produce any terminal label in the contralateral OPt (not shown), but did produce an extensive plexus of labeled axons (arrows) in the adjacent ipsilateral OPt (**h**) (box in **g** indicates the location of **h**). Scale in **h** = **d**, **f**, **c** = **g**, Scale bar in inset **c** = 1.0 mm, **e** = 500 µm, and **f** = 100 µm

unknown, as OPt cell responses have only been tested with respect to visual sensory inputs. As such, they may represent an interesting future avenue of investigation.

Acknowledgements We would like to thank Ms. Malinda Danielson, Jinrong Wei, and Olga Golanov for their technical assistance with respect to surgeries and processing of the brains, as well as preparation of the figures. We are also indebted to Mr. Glen Hoskins for processing and cutting tissue for electron microscopy.

Author contributions PJM helped to: design the experiments, carry out the experiments, analyze the data, write the manuscript, and edit the manuscript. SW helped to: carry out the experiments, analyze the data, and edit the manuscript.

Funding Portions of the material presented here were supported by funds from National Institute of Health grants: EY07166 to Paul J. May, EY014263 to Paul J. May, Paul D.R. Gamlin, and Susan Warren,

and National Science Foundation Grant IBN-0130954 to Martha Bickford and Paul J. May.

Compliance with ethical standards

Conflict of interest Neither author has any perceived or real conflicts of interest with respect to this submission.

Ethical use of animals statement All applicable international, national, and/or institutional guidelines for the care and use of animals were followed. All procedures performed in studies involving animals were in accordance with the ethical standards of the institution at which the studies were conducted. Specifically, they were undertaken under protocols approved by the Institutional Animal Care and Use Committee of the University of Mississippi Medical Center (USDA Animal Welfare Assurance # D16-00174).

References

Baleydier C, Magnin M, Cooper HM (1990) Macaque accessory optic system: II. Connections with the pretectum. J Comp Neurol 302:405–416

Barnerssoi M, May PJ (2016) Postembedding immunohistochemistry for inhibitory neurotransmitters in conjunction with neuroanatomical tracers. In: Van Bockstaele EJ (ed) Transmission electron microscopy methods for understanding the brain. Neuromethods, vol 115. Springer Science, New York, pp 181–203

Berson DM, Dunn FA, Takao M (2002) Phototransduction by retinal ganglion cells that set the circadian clock. Science 295:1070–1073

Campbell G, Lieberman AR (1982) Synaptic organization in the olivary pretectal nucleus of the adult rat. Neurosci Lett 28:151–155

Campbell G, Lieberman AR (1985) The olivary pretectal nucleus: experimental anatomical studies in the rat. Philos Trans R Soc Lond B Biol Sci 310:573–609

Chen B, May PJ (2000) The feedback circuit connecting the superior colliculus and central mesencephalic reticular formation: a direct morphological demonstration. Exp Brain Res 131:10–21

Clarke RJ, Ikeda H (1985a) Luminance detectors in the olivary pretectal nucleus and their relationship to the pupillary light reflex in the rat. II. Studies using sinusoidal light. Exp Brain Res 59:83–90

Clarke RJ, Ikeda H (1985b) Luminance and darkness detectors in the olivary and posterior pretectal nuclei and their relationship to the pupillary light reflex in the rat. I. Studies with steady luminance levels. Exp Brain Res 57:224–232

Clarke RJ, Blanks RH, Giolli RA (2003a) Midbrain connections of the olivary pretectal nucleus in the marmoset (*Callithrix jacchus*): implications for the pupil light reflex pathway. Anat Embryol (Berl) 207:149–155

Clarke RJ, Zhang H, Gamlin PD (2003b) Primate pupillary light reflex: receptive field characteristics of pretectal luminance neurons. J Neurophysiol 89:3168–3178

Distler C, Hoffmann KP (1989) The pupillary light reflex in normal and innate microstrabismic cats, I: behavior and receptive-field analysis in the nucleus praetectalis olivaris. Vis Neurosci 3:127–138

Fukuda Y, Stone J (1974) Retinal distribution and central projections of Y-, X-, and W-cells of the cat's retina. J Neurophysiol 37:749–772

Gamlin PDR (2006) The pretectum: connections and oculomotor-related roles. Prog Brain Res 151:379–405

Gamlin PD, Clarke RJ (1995) The pupillary light reflex pathway of the primate. J Am Opt Assoc 66:415–418

Gamlin PD, Cohen DH (1988) Retinal projections to the pretectum in the pigeon (*Columba livia*). J Comp Neurol 269:1–17

Gamlin PD, Reiner A, Erichsen JT, Karten HJ, Cohen DH (1984) The neural substrate for the pupillary light reflex in the pigeon (*Columba livia*). J Comp Neurol 226:523–543

Gamlin PD, Zhang H, Clarke RJ (1995) Luminance neurons in the pretectal olivary nucleus mediate the pupillary light reflex in the rhesus monkey. Exp Brain Res 106:169–176

Gerfen CR, Sawchenko PE (1984) An anterograde neuroanatomical tracing method that shows the detailed morphology of neurons, their axons and terminals: immunohistochemical localization of an axonally transported plant lectin, Phaseolus vulgaris leucoagglutinin (PHA-L). Brain Res 290:219–238

Gregory KM (1985) The dendritic architecture of the visual pretectal nuclei of the rat: a study with the Golgi-Cox method. J Comp Neurol 234:122–135

Hannibal J, Kankipati L, Strang CE, Peterson BB, Dacey D, Gamlin PD (2014) Central projections of intrinsically photosensitive retinal ganglion cells in the macaque monkey. J Comp Neurol 522:2231–2248

Hattar S, Liao HW, Takao M, Berson DM, Yau KW (2002) Melanopsin-containing retinal ganglion cells: architecture, projections, and intrinsic photosensitivity. Science 295:1065–1070

Hoffmann KP, Ballas I, Wagner HJ (1984) Double labelling of retinofugal projections in the cat: a study using anterograde transport of 3H-proline and horseradish peroxidase. Exp Brain Res 53:420–430

Hutchins B, Weber JT (1985a) The pretectal complex of the monkey: a reinvestigation of the morphology and retinal terminations. J Comp Neurol 232:425–442

Hutchins B, Weber JT (1985b) The pretectal olivary nucleus of the cat: evidence for a two-tailed structure. Brain Res 331:150–154

Klooster J, Vrensen GF (1997) The ultrastructure of the olivary pretectal nucleus in rats. A tracing and GABA immunohistochemical study. Exp Brain Res 114:51–62

Klooster J, van der Want JJ, Vrensen G (1983) Retinopretectal projections in albino and pigmented rabbits: an autoradiographic study. Brain Res 288:1–12

Klooster J, Vrensen GF, Müller LJ, van der Want JJ (1995) Efferent projections of the olivary pretectal nucleus in the albino rat subserving the pupillary light reflex and related reflexes. A light microscopic tracing study. Brain Res 688:34–46

Klooster J, Kamphuis W, Vrensen GF (2000) Immunohistochemical localization of substance P and substance P receptor (NK1) in the olivary pretectal nucleus of the rat. Exp Brain Res 131:57–63

Liao HW, Ren X, Peterson BB, Marshak DW, Yau KW, Gamlin PD, Dacey DM (2016) Melanopsin-expressing ganglion cells in macaque and human retinas form two morphologically distinct populations. J Comp Neurol 524:2845–2872

Lieberman AR, Taylor AM, Campbell G (1985) Axon terminals of the projection from the superior colliculus to the olivary pretectal nucleus in the rat. Neurosci Lett 56:235–239

May PJ, Sun W, Hall WC (1997) Reciprocal connections between the zona incerta and the pretectum and superior colliculus of the cat. Neuroscience 77:1091–1114

May PJ, Sun W, Erichsen JT (2008) Defining the pupillary component of the perioculomotor preganglionic population within a unitary primate Edinger-Westphal nucleus. In: Kennard C, Leigh RJ (eds) Using eye movements as an experimental probe of brain function, Prog Brain Res, vol 171, pp 97–106

May PJ, Warren S, Gamlin PDR, Billig I (2018) An anatomic characterization of the midbrain near response neurons in the macaque monkey. Invest Ophthalmol Vis Sci 59:1486–1502

May P J, Reiner A, Gamlin PD (2019) Autonomic regulation of the eye. In: Encyclopedia of neuroendocrine and autonomic systems. In: Nelson R (ed). Oxford University Press, Oxford

Miguel-Hildago JJ, Senba E, Takatsuji K, Tohyama M (1994) Projections of takykinin- and glutaminase-containing rat retinal ganglion cells. Brain Res Bul 35:73–84

Mustari MJ, Fuchs AF, Kaneko CR, Robinson FR (1994) Anatomical connections of the primate pretectal nucleus of the optic tract. J Comp Neurol 349:111–128

Olucha F, Martínez-García F, López-García C (1985) A new stabilizing agent for the tetramethyl benzidine (TMB) reaction product in the histochemical detection of horseradish peroxidase (HRP). J Neurosci Methods 13:131–138

Ostrin LA, Strang CE, Chang K, Jnawali A, Hung LF, Arumugam B, Frishman LJ, Smith EL 3rd, Gamlin PD (2018) Immunotoxin-induced ablation of the intrinsically photosensitive retinal ganglion cells in rhesus monkeys. Front Neurol 9:1000

Pong M, Fuchs AF (2000) Characteristics of the pupillary light reflex in the macaque monkey: discharge patterns of pretectal neurons. J Neurophysiol 84:964–974

Scalia F (1972) Retinal projections to the olivary pretectal nucleus in the tree shrew and comparison with the rat. Brain Behav Evol 6:237–252

Scalia F, Arango V (1979) Topographic organization of the projections of the retina to the pretectal region in the rat. J Comp Neurol 186:271–292

Scalia F, Rasweiler JJ 4th, Danias J (2015) Retinal projections in the short-tailed fruit bat, *Carollia perspicillata*, as studied using the axonal transport of cholera toxin B subunit: comparison with mouse. J Comp Neurol 523:1756–1791

Schmidt TM, Do MT, Dacey D, Lucas R, Hattar S, Matynia A (2011) Melanopsin-positive intrinsically photosensitive retinal ganglion cells: from form to function. J Neurosci 31:16094–16101

Simpson JI, Giolli RA, Blanks RH (1988) The pretectal nuclear complex and the accessory optic system. Rev Oculomot Res 2:335–364

Steiger HJ, Büttner-Ennever JA (1979) Oculomotor nucleus afferents in the monkey demonstrated with horseradish peroxidase. Brain Res 160:1–15

Sun W, May PJ (1995) Morphology and connections of the pupillary light reflex pathway in cat and monkey. Invest Ophthal Vis Sci 36:S12

Sun W, May PJ (2014a) Central pupillary light reflex circuits in the cat: I. The olivary pretectal nucleus. J Comp Neurol 522:3960–3977

Sun W, May PJ (2014b) Central pupillary light reflex circuits in the cat: II. Morphology, ultrastructure, and inputs of preganglionic motoneurons. J Comp Neurol 522:3978–4002

Trejo LJ, Cicerone CM (1984) Cells in the pretectal olivary nucleus are in the pathway for the direct light reflex of the pupil in the rat. Brain Res 300:49–62

Weber JT, Young R, Hutchins B (1981) Morphologic and autoradiographic evidence for a laminated pretectal olivary nucleus in the squirrel monkey. Brain Res 224:153–159